

Griffiths Effects in Random Heisenberg Antiferromagnetic $S = 1$ Chains

Kedar Damle

Physics Department, Harvard University, Cambridge, MA 02138

(January 7, 2002)

I consider the effects of enforced dimerization on random Heisenberg antiferromagnetic $S = 1$ chains. I argue for the existence of novel Griffiths phases characterized by *two independent dynamical exponents* that vary continuously in these phases; one of the exponents controls the density of spin-1/2 degrees of freedom in the low-energy effective Hamiltonian, while the other controls the corresponding density of spin-1 degrees of freedom. Moreover, in one of these Griffiths phases, the system has very different low temperature behavior in two different parts of the phase which are separated from each other by a sharply defined crossover line; on one side of this crossover line, the system ‘looks’ like a $S = 1$ chain at low energies, while on the other side, it is best thought of as a $S = 1/2$ chain. A strong-disorder RG analysis makes it possible to analytically obtain detailed information about the low temperature behavior of physical observables such as the susceptibility and the specific heat, as well as identify an experimentally accessible signature of this novel crossover.

I. INTRODUCTION

Quantum spin chain systems are known to exhibit many interesting states of matter at low temperature that arise from the fascinating interplay between quantum fluctuations, correlation effects, and the effects of quenched disorder. They are particularly interesting from a theoretical point of view, as they provide experimentally realizable examples in which this interplay, common to many other condensed-matter systems, can be studied in detail.

Among the most studied such systems is the Heisenberg antiferromagnetic (HAF) $S = 1$ chain (for an experimental review see Ref. 1) with Hamiltonian:

$$\mathcal{H} = J \sum_i \hat{S}_i \cdot \hat{S}_{i+1}, \quad (1)$$

where J is positive, and the operators \hat{S} represent the spin angular momentum of spin-1 objects on site i of a one-dimensional lattice. As Haldane² showed many years ago, quantum fluctuations in the $S = 1$ HAF chain are strong enough to rule out even quasi-long range antiferromagnetic order of the type present in $S = 1/2$ chains, and the system is in the so-called ‘Haldane’ phase characterized by a singlet ground-state and gap to all bulk excitations. However, this phase possesses a kind of ‘topological’ order³ that results in the presence of almost free sub-gap boundary spin-1/2 degrees of freedom in a large but finite system of length L with free ends; these spin-1/2s are coupled to each other by an effective exchange coupling $J_{\text{eff}} \sim (-1)^{L+1} e^{-cL}$ (with L in lattice units, and c proportional to the inverse ground-state correlation length), and will play a crucial role in much of the analysis in this paper.

A very intuitive and useful picture of the Haldane phase is the ‘valence-bond’ solid⁴ description: The basic idea is to think of each spin-1 as a (symmetrized) pair of spin-1/2 objects; each site thus has two ‘indistinguishable’ spin-1/2 objects on it. A good description of the

ground state is then obtained by pairing one of the spin-1/2 at any site into a singlet state with a spin-1/2 on its neighbor to the right, and pairing the other spin-1/2 into a singlet state with a spin-1/2 on its neighbor to the left. This gives a state with one singlet bond across each link of the lattice, i.e the (1,1) state. The topological order present in the Haldane phase can now be thought of simply as the ability to ‘walk’ across the length of the system along singlet bonds without encountering any breaks, and the unpaired spin-1/2s at each end of a chain with free boundaries model the sub-gap end-states characteristic of the Haldane phase.

The stability of this phase to various experimentally relevant perturbations has also been investigated. For instance, it is known⁵ that the Haldane phase is stable to weak enforced dimerization δ in the exchange couplings (δ parametrizes the extent to which the even bonds are stronger than the odd bonds), and there are no qualitative differences in the low-energy properties of the system until $|\delta|$ exceeds a critical value δ_c . Beyond this point, the ground state changes character, and the system enters a different gapped state without the topological order or the subgap spin-1/2s on free ends. For positive $\delta > \delta_c$, this dimerized phase corresponds to the (2,0) valence-bond state in which both spin-1/2 degrees of freedom at any even-numbered physical site form singlets with spin-1/2s on its neighbor to its right, and the number of singlet bonds across each link of the lattice alternates between two and zero (similarly, the (0,2) state is favored by the system when $\delta < -\delta_c$).

The effects of quenched randomness R in the exchange couplings (with all J_i still positive) have also been studied^{6,7} at $\delta = 0$ (in the presence of randomness, δ is defined in terms of the average values for even and odd bonds). The topological order characteristic of the Haldane state persists for R less than a critical value R_c , and the Haldane phase is thus stable to weak randomness. On the other hand, a different, randomness dominated state is stabilized for $R > R_c$. In this ‘Spin-1 Random Singlet’ (RS₁) state, the interplay of disorder and quantum me-

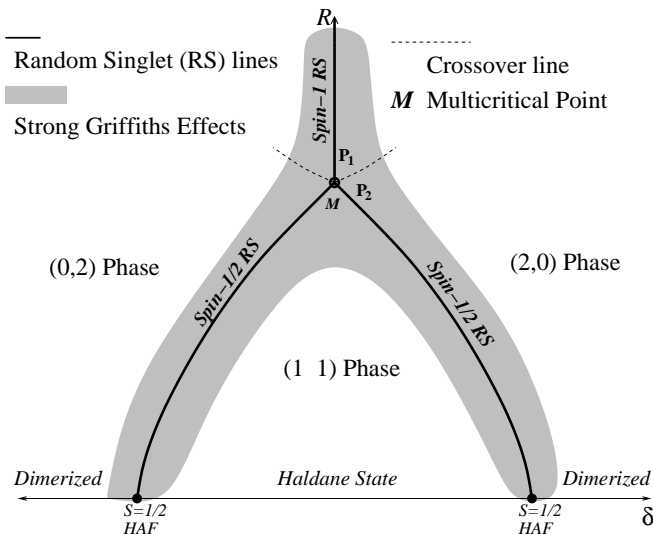


FIG. 1. Schematic phase diagram as a function of randomness (R) and dimerization (δ). Details in text

chanics locks each spin-1 into a singlet state with some other spin-1; the two spins in a given singlet pair can have arbitrarily large spatial separation, with disorder determining the actual choice of partner for each spin;⁸ in the valence bond picture, this large R state is thus characterized by a particular *random* pattern of *double* bonds.

Although the topological order survives for all $R < R_c$, it turns out that disorder has a dramatic effect on the low-energy properties near the transition, resulting in arbitrarily low-energy excitations with a power-law density of states controlled by a single non-universal (R dependent) *dynamical exponent* z . These low-energy excitations are associated with large anomalous regions of the sample in which the couplings locally favor a pattern of singlet bonds more characteristic of the other ‘nearby’ phase(s) (see below). Such ‘Griffiths effects’, whereby rare disorder-induced fluctuations in the interactions over extended regions of space give rise to *non-universal* singular contributions that dominate low-energy properties, are among the more interesting and ubiquitous aspects of the physics of low-dimensional random quantum systems, and below, I focus on precisely this physics for the general $\delta \neq 0$ case.

II. PHYSICAL PICTURE AND MOTIVATION

Let us start with the overall structure of the phase diagram in the (R, δ) plane: To begin with, note that the nature of the ground state will not change qualitatively from that at $\delta = 0$ as long as $R < R_c$ and δ is small enough. On the other hand, by analogy with the corresponding situation in random HAF $S = 1/2$ chains,¹⁴ the RS_1 state for $R > R_c$ will be unstable to adding a tiny amount of dimerization. For small $\delta > 0$, the resulting

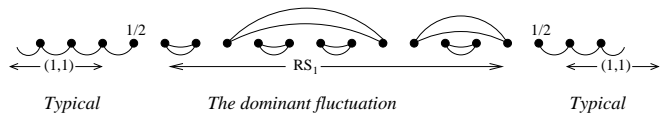


FIG. 2. A cartoon for Griffiths effects in the Gapless Haldane phase at $\delta = 0$

pattern of singlet bonds in the ground state will be the random analog of the $(2,0)$ state of the pure system, and topologically indistinguishable from the latter. Likewise, the state for infinitesimal $\delta < 0$ will be topologically identical to the $(0,2)$ state. Putting all this together, we are led to a phase diagram that looks something like the one sketched in Fig 1. The critical point^{6,7} at $R = R_c, \delta = 0$ is thus really a *multicritical point* at which the $(2,0)$, $(0,2)$ and $(1,1)$ phases meet, while the RS_1 line is seen to be the critical phase boundary between the $(0,2)$ and $(2,0)$ phases.

To complete this part of our discussion, we need to identify the universality class of the phase-boundary between the $(1,1)$ phase and either of the dimerized phases. To this end, note that the physics asymptotically close to $\pm\delta_c$ at $R = 0$ is that of a *spin-1/2* chain with a small value of enforced dimerization: heuristically, this may be understood by first putting down a single valence bond on each even link (for $\delta > 0$) to partially ‘screen’ out the imbalance in the odd and even exchange couplings; this leaves behind a $S = 1/2$ HAF chain with $\delta_{\text{eff}} \sim \delta - \delta_c$. Now, we know⁸ that adding disorder to the $S = 1/2$ HAF at $\delta_{\text{eff}} = 0$ leads to a spin-1/2 Random Singlet ($RS_{1/2}$) state (with a random pattern of *single* valence bonds statistically identical to the pattern of *double* bonds in the RS_1 phase), and thus, the $\delta \neq 0$ phase boundaries between the $(1,1)$ state and the $(2,0)$ or $(0,2)$ states are lines along which the system is in the $RS_{1/2}$ critical state.

Of course, the topological labels of the different phases and the universality classes of various transitions are not the whole story, and we need to consider the role of Griffiths effects in various regimes to really understand the low-energy behavior of the phases. Consider, for starters, the Gapless Haldane regime at $\delta = 0$. The gapless spectrum obtained in Refs 6,7 can be understood by thinking about the effect of a single rare region of length L in which the exchange couplings are such that the preferred pattern of singlet bonds in this region is more characteristic of a system at a nearby point in either the random $(2,0)$ or $(0,2)$ phases, or on the critical RS_1 line separating them (outside of this rare segment of length L , the system is in the ‘typical’ $(1,1)$ state). In all such cases, the central segment (see Fig 2) can be thought of as an ‘insulating’ barrier that separates two essentially semi-infinite chains in the Haldane phase, implying the presence of low-energy spin-1/2 degrees of freedom localized at the ends of the $(1,1)$ segments.

These spin-1/2s are coupled to each other across the ‘barrier’ by an antiferromagnetic exchange coupling of order $e^{-c_1 L}$, while the probability for such an anoma-

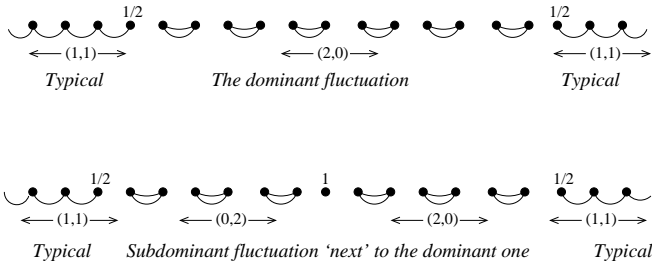


FIG. 3. A caricature of Griffiths effects in the (1,1) phase at positive δ

lous disorder configuration to occur is also exponentially small: $p_L \sim e^{-c_2 L}$. Averaging over different possibilities, with anomalous regions of varying length $L \gtrsim -\ln(\Omega)/c_1$, then yields a power-law for the density of spin-1/2 degrees of freedom that model the physics below the energy scale Ω : $n_{1/2} \sim \Omega^{1/z}$, with a non-universal exponent z (here, and henceforth, Ω denotes some suitable low energy scale much smaller than the microscopic scale J_{typ}). Now, if two such anomalous regions occur essentially ‘next’ to each other (*i.e.* separated by a segment with typical exchange couplings of length $L \lesssim -\ln(\Omega)$), and if L is *even*, then the end spin-1/2 degrees of freedom of this intervening typical segment will bind ferromagnetically to each other producing an effective spin-1 as far as the low-energy dynamics below the cutoff scale Ω is concerned. The probability for this to happen is dominated by the requirement that two anomalous regions, that are usually separated by lengths of order $\Omega^{-1/z}$, occur essentially next to each other—this immediately implies that the density of spin-1 degrees of freedom in the effective Hamiltonian will scale as the square of the density of spin-1/2 objects, consistent (apart from a log-correction) with the RG results of Ref 6.

It turns out that similar heuristic arguments can be employed to qualitatively understand Griffiths effects at $\delta > 0$ in the (1,1) phase, *i.e.* closer to the phase boundary to the (2,0) state (see fig 3): In this case, the dominant disorder-induced fluctuation will consist of large regions of the sample that locally want to be in the (2,0) state—the probability of their occurrence will control the exponent $z_{1/2}$ that determines the density $n_{1/2} \sim \Omega^{1/z_{1/2}}$ of low-energy spin-1/2 degrees of freedom below scale Ω , while much rarer regions that locally prefer the (0,2) phase or the RS_1 critical state will only provide subdominant corrections as far as the value of $z_{1/2}$ is concerned.

However, it is clearly impossible (simply for parity reasons) to have two anomalous segments in the (2,0) phase separated from each other by an *even* segment—one of these anomalous regions necessarily has to be of a much rarer sub-dominant type (either a (0,2) region, or one with a spin-1 random singlet pattern of valence bonds) in such a situation. These are precisely the configurations that behave at low energies as a spin-1 object, and thus, the spatial density of spin-1 degrees of freedom below

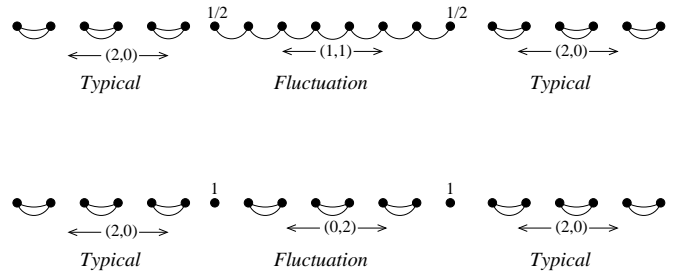


FIG. 4. Cartoon for Griffiths effects in the (2,0) phase

scale Ω vanishes faster than $\Omega^{2/z_{1/2}}$. Introducing a second exponent $z_1 \leq z_{1/2}/2$ to describe this behavior, we therefore arrive at $n_1 \sim \Omega^{1/z_1}$. Moreover, it is also clear from this argument that $z_{1/2}$ will diverge as we approach the transition at non-zero δ into either the (2,0) or (0,2) phases (after all, what was the dominant rare fluctuation becomes the typical configuration as one crosses the transition!), while z_1 , whose value near the $\text{RS}_{1/2}$ phase boundary is primarily determined by the *sub-dominant* fluctuation, will remain finite at this transition.

In this analysis of the (1,1) phase, I have been unavoidably led to a description in terms of *two independent* dynamical exponents. This is, of course, formally quite interesting—however, since $z_1 \leq z_{1/2}/2$ throughout this phase, this additional ‘tuning-knob’ does not lead to any qualitative changes in the low-energy physics as we move around in this phase. On the other had, the situation in the (2,0) (or (0,2)) phase in the vicinity of its phase boundaries is dramatically different, and this is what I turn to next.

To begin with, let us focus on two representative points in this phase (see Fig 1), lying on an arc drawn around the multicritical point and going from the RS_1 critical line to the $\text{RS}_{1/2}$ critical line. Consider first the point P_1 very close to the RS_1 line: The low-energy dynamics at this point will be dominated by rare large regions that locally want to be at a nearby point in the (0,2) phase, embedded in a more typical background which is in the (2,0) phase (see fig 4). Such an anomalous region clearly has residual spin-1 objects at either end, and the low-energy dynamics below scale Ω will be dominated by a density $n_1 \sim \Omega^{1/z_1}$ of these, with z_1 being controlled by the probability for such anomalies to occur at the corresponding length scales.

Of course, there will also be sub-dominant disorder fluctuations that involve much rarer regions locally in the (1,1) phase; these have spin-1/2 degrees of freedom at their ends, and the low-energy dynamics will therefore also have sub-dominant contributions from a density $n_{1/2} \sim \Omega^{1/z_{1/2}}$ of these (with $z_{1/2} \ll z_1$ being controlled by the probability of occurrence for the (1,1) anomalies). Simply put, in this regime of the (2,0) phase, the low-energy behavior is more or less that of a spin-1 system. Next, consider the point P_2 chosen very close to the $\text{RS}_{1/2}$ phase boundary. The situation is now completely re-

versed, and the dominant Griffiths effects arise from rare regions locally at a nearby point in the (1,1) phase. Thus, $z_{1/2}$ will be much larger than z_1 in this regime, and the low-energy behavior is predominantly that of a system made up of spin-1/2 objects.

Clearly, as we move along the arc from P_1 to P_2 , the low-energy response will smoothly interpolate between these two extremes. Thus, the system in either the (2,0) or (0,2) phase has a curious ability to look *qualitatively different at low energies* in different parts of the phase, undergoing a metamorphosis from a spin-1/2 system into a spin-1 system as we move around in the phase. In particular, one expects that there will be some intermediate point along the arc at which $z_1 = z_{1/2}$; at this point, *both* spin-1/2 and spin-1 degrees of freedom will play a role in determining the low-energy behavior of the system. [More generally, one expects a crossover line emanating from the multicritical point, along which $n_{1/2} \sim n_1 \sim \Omega^{1/z}$ as $\Omega \rightarrow 0$.]

These heuristic considerations clearly demonstrate that there is enough new and interesting physics at $\delta \neq 0$ to warrant a more serious analysis, and this is what I turn to next.

III. EFFECTIVE MODEL AND THE RG APPROACH

To go beyond the qualitative arguments of the previous section, one needs to analyze an appropriate effective model in a controlled manner. To fix the form of this effective model, it is useful to specialize to a situation in which the bonds J_i in our Hamiltonian

$$\mathcal{H} = \sum_i J_i \hat{S}_i \cdot \hat{S}_{i+1} \quad (2)$$

only take values 1, $\epsilon_s > 0$, or $\epsilon_w > 0$ (s and w stand for ‘strong’ and ‘weak’, with $1 > \epsilon_s > \epsilon_w$). For i even, J_i is 1 with probability $1 - p_s$ (the J_i for i even are thus ‘strong’), and ϵ_s with probability p_s , while, for i odd, J_i is 1 with probability $1 - p_w$ (the J_i for odd i are thus ‘weak’), and ϵ_w with probability p_w (with $p_w > p_s$). For concreteness, it is also useful to take the p_s/w and ϵ_s/w all much smaller than 1. In this case, it is appropriate to think in terms of a collection of fairly large segments of a pure $S = 1$ HAF chain in the Haldane state, coupled to each other by the ϵ -bonds, and described in terms of pairs of the sub-gap boundary spin-1/2 degrees of freedom at their ends.

Given that $p_w > p_s$, a typical segment of this kind will be, more likely than not, flanked on *both* sides by ϵ_w -bonds. Consequently, such a segment will be *odd in length*, and its low-energy behavior will be described by a pair of spin-1/2s coupled to each other by an ‘odd’ bond which is *antiferromagnetic*, and drawn from a distribution that is calculable in terms of the length-distribution of the pure segments (the designation ‘odd’ has nothing

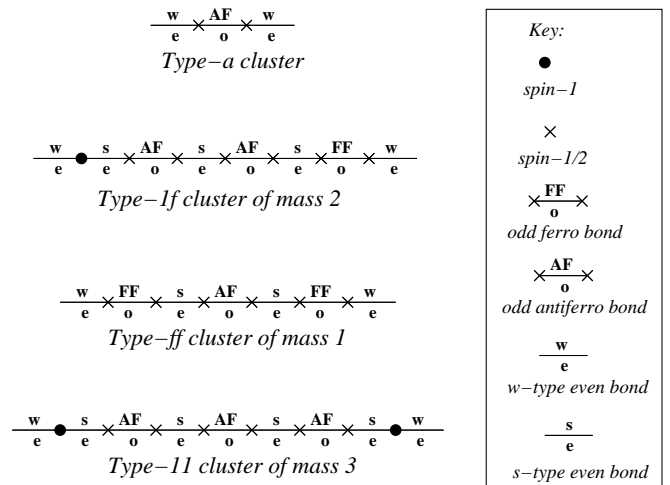


FIG. 5. Some examples of the different types of clusters that make up our effective model.

to do with the parity of the segment length, and is chosen to conform to the notation of Ref. 6 when $\delta = 0$)—the bonds connecting this ‘odd’ pair to the rest of the system on either side are ‘even’ bonds of the w -type (the designation ‘even’ is again chosen to conform with Ref 6 when $\delta = 0$; clearly all ‘even’ bonds are always antiferromagnetic). On the other hand, a segment flanked on one side by an ϵ_s -bond, and on the other by a ϵ_w bond, will be *even in length*, and its low-energy description will consist of a pair of spin-1/2s coupled by a *ferromagnetic* ‘odd’ bond (whose *modulus* has the same distribution as in the earlier antiferromagnetic case). Of course, this odd ferromagnetic pair is flanked by one s -type even bond and another w -type even bond; odd ferromagnetic bonds thus have a s -flank and a w -flank.

Moreover, and this is crucial, the other ϵ -bonds in the vicinity of any such segment (that contributes a ferromagnetically coupled odd pair of spin-1/2s to the effective model) are again *more likely to be of the w-type*, and thus, there is an enhanced probability for finding another even-length pure segment (contributing *another* pair of spin-1/2 coupled by a *ferromagnetic* odd bond) close-by on the s -flank of this segment. In other words, a ferromagnetic odd bond in the effective theory likes to have another ferromagnetic odd bond (or a spin-1 object; see below) close-by on its s -flank. Likewise, an odd-length segment flanked on *both* sides by ϵ_s bonds (described at low-energies by an odd antiferromagnetic pair of spin-1/2s flanked on both sides by s -type even bonds) is more likely than not to have nearby even-length segments in the Haldane phase; thus, in the effective theory, an odd antiferromagnetic bond flanked by s -type even bonds on *both* sides side likes to have odd ferromagnetic bonds (or spin-1s; see below) close by on *both* sides. Finally, two ϵ bonds right next to each other will give rise to a spin-1 object connected to the rest of the system by a w -type even bond on one side, and a s -type even bond on the

other (obviously, such a spin-1 object also has a tendency to have another ferromagnetic odd bond (or spin-1) close-by on its s -flank). Clearly, one could equally well represent this spin-1 by two spin-1/2s connected by a ferromagnetic odd bond with strength much bigger than the cutoff,^{6,7} and in this sense, this is just a special case of a ferromagnetically coupled odd-pair—however, I prefer to explicitly introduce spin-1 objects into my description here.

This dimerization induced clustering tendency of the ferromagnetically coupled odd pairs (or spin-1s) in the effective model immediately implies that individual pairs of spin-1/2s coupled by odd bonds (and their special case: spin-1s) are not the elementary constituents of our effective theory (this should be contrasted with the $\delta = 0$ case, where the low-energy effective model does consist of statistically independent odd pairs coupled together by even bonds).⁶ Clearly, the solution is to think not in terms of individual odd pairs, but in terms of *clusters*: The simplest cluster, the a -type cluster, is just a pair of spin-1/2s coupled by an *antiferromagnetic* odd bond, and flanked on both sides by w -type even bonds. Any other cluster of mass μ is made up of a string of μ antiferromagnetically coupled odd pairs of spin-1/2s ($\mu = 0, 1, 2, 3 \dots$), each flanked by s -type even bonds on both sides (the total number of s -type even bonds is thus $\mu + 1$), terminating at each end in a ferromagnetically coupled odd pair of spin-1/2s. Of course, either, or both, of the terminating pairs could equally well be replaced by a single spin-1 each, and there are thus three kinds of clusters: 11 (with two spin-1s at the two ends), $1f$ (with a spin-1 at one end and a pair of spin-1/2s coupled with an odd ferromagnetic bond at the other end), and ff (with ferromagnetically coupled odd pairs of spin-1/2s at both ends).

Our effective model¹¹ is thus made up of these four types of statistically independent clusters, connected to each other by intervening w -type even bonds. Furthermore, the absolute values of all odd bonds, regardless of their sign, are expected to be governed by a single distribution P_o . On the other hand, the w -type and s -type even bonds will have two different distributions, which we denote by P_w and P_s respectively. Furthermore, since each end of any cluster is expected to independently be either a spin-1, or a ferromagnetically coupled odd pair of spin-1/2s, the relative abundances of the 11 , $1f$, and ff clusters can be parametrized by a single probability g for an end to be a spin-1 (with the probability for an end to be a ferromagnetically coupled pair of spin-1/2s being $1 - g$). Similarly, the density of the ‘elementary’ a -type clusters relative to the density of all other clusters can be parametrized by a probability f_a for any given cluster to be of type a . Finally, since we are dealing with uncorrelated disorder, it is reasonable to expect that the masses μ of the 11 , $1f$, and ff clusters are all characterized by a single exponential distribution, with probability $\propto q^\mu$ for any cluster to have mass μ .

All these expectations are borne out by my detailed

calculations below; for now, I only note that the effective model is completely specified by the three probabilities g , f_a and q , the three probability distributions P_s , P_w and P_o , and the number of w -type even bonds N_w . Naturally, the initial values of these parameters and distributions (at the intermediate energy scale Ω_0 below which this model becomes applicable) are determined by the complicated interplay of dimerization and randomness in the microscopic model—fortunately, their precise values and functional forms will, for the most part, be unimportant as far as the physics at scales $\Omega \ll \Omega_0$ is concerned.

To get at this low-energy physics, it is convenient to use a strong-disorder RG approach^{6,8,9} in which we iteratively diagonalize the most strongly coupled parts of the Hamiltonian: Thus, at each step, we focus on the strongest bond $|J_{\max}| \equiv \Omega$ in the system. Consider, first, the case when this is an antiferromagnetic bond: If this bond connects two spin-1/2s (such a bond can clearly be either even or odd), we freeze the two spin-1/2s into a singlet state, and introduce a renormalized coupling between the neighboring spins on either side: $\tilde{J} = J_L J_R / J_{\max}$; here J_L and J_R are the bonds immediately adjacent to J_{\max} , respectively to its left and to its right. If this bond connects two spin-1s (in this case, J_{\max} must necessarily be an even bond), we again freeze them into their singlet ground state, and couple the neighboring spins on either side to each other with the renormalized bond $\tilde{J} = J_L J_R / J_{\max}$. Finally, consider the case where J_{\max} couples a spin-1 with a spin-1/2 (again, in this case, J_{\max} must be even), with this spin-1/2 coupled to its other neighbor with a bond J_{half} , and this spin-1 coupled to its other neighbor with a bond J_{one} . In this case, we form a renormalized spin-1/2 object representing the doublet ground state of this pair. The neighboring bonds J_{half} and J_{one} remain unchanged in magnitude after the RG step, but J_{half} *changes sign*. Finally, if J_{\max} is ferromagnetic (in this case, J_{\max} has to be an odd bond connecting two spin-1/2s), we put this pair of spin-1/2s into their triplet ground state, and replace it by an equivalent spin-1.

This formulation of the RG is completely equivalent to the one used in Ref 6, and ignores $O(1)$ coefficients in the RG recursion relations as well as the distinction between the bond J coupling a pair, and the gap in its spectrum—as in that case, I expect it to give accurate results when the effective value of disorder in the low-energy theory is large. My calculations will therefore be essentially exact in the regime of strong Griffiths effects (with a large value for at least one of the dynamical exponents), and are expected to be accurate even for smaller values of the dynamical exponents.¹⁵ In the next two sections, I use this RG approach to analyze the low-energy physics of the effective model.

IV. RG FLOW-EQUATIONS AND FIXED-POINTS

It is straightforward, if a little tedious, to write down the flow equations that describe the iterated action of the RG rules on our effective model, and this is what I turn to next.

But first, some additional notation: Let us introduce $N_{ff}(\mu)$, $N_{1f}(\mu)$, $N_{11}(\mu)$, and N_a to denote the number of mass- μ ff , $1f$, 11 clusters, and a -type clusters respectively. Thus, we have

$$\begin{aligned} N_{ff}(\mu) &= (1 - f_a)(1 - g)^2(1 - q)q^\mu N_w, \\ N_{1f}(\mu) &= 2(1 - f_a)g(1 - g)(1 - q)q^\mu N_w, \\ N_{11}(\mu) &= (1 - f_a)g^2(1 - q)q^\mu N_w, \\ N_a &= f_a N_w. \end{aligned} \quad (3)$$

In addition, let us denote the total number of ff , $1f$, and 11 clusters by N_{ff} , N_{1f} , and N_{11} respectively. It is also convenient to introduce the log-cutoff $\Gamma = \ln(\Omega_0/\Omega)$, and the log-couplings $\beta = \ln(\Omega/|J|)$, and keep track of the probability distributions of bond-strengths in terms of the probability distributions $P_{s/o/w}(\beta|\Gamma)$ of the corresponding log-couplings. And finally, let us introduce $P_{s/o/w}^0(\Gamma)$ to refer to $P_{s/w/o}(0|\Gamma)$ respectively.

The flow equations for the probabilities read

$$\begin{aligned} \frac{df_a}{d\Gamma} &= (1 - f_a)[P_s^0(1 - q)(1 - g^2(1 - f_a)) - f_a(P_o^0 + P_w^0)], \\ \frac{dq}{d\Gamma} &= (1 - q)[P_w^0(1 - f_a)(1 - g^2(1 - q)) - q(P_o^0 + P_s^0)], \\ \frac{dg}{d\Gamma} &= (1 - g)P_o^0 - g(P_s^0 q + P_w^0 f_a), \end{aligned} \quad (4)$$

while those for the functions $P_{s/w/o}$ read:

$$\begin{aligned} \frac{\partial P_s}{\partial \Gamma} &= \frac{\partial P_s}{\partial \beta} + P_s^0 P_s + \\ &+ (qP_o^0 + (1 - q)(1 - f_a)g^2 P_w^0)(P_s \otimes P_s - P_s), \\ \frac{\partial P_w}{\partial \Gamma} &= \frac{\partial P_w}{\partial \beta} + P_w^0 P_w + \\ &+ (f_a P_o^0 + (1 - q)(1 - f_a)g^2 P_s^0)(P_w \otimes P_w - P_w), \\ \frac{\partial P_o}{\partial \Gamma} &= \frac{\partial P_o}{\partial \beta} + P_o^0 P_o + \\ &+ (AP_s^0 + BP_w^0)(P_o \otimes P_o - P_o), \end{aligned} \quad (5)$$

where $P \otimes P$ stands for the convolution

$$P \otimes P = \int_0^\infty \int_0^\infty d\beta_1 d\beta_2 P(\beta_1|\Gamma)P(\beta_2|\Gamma)\delta(\beta - \beta_1 - \beta_2),$$

and $A(\Gamma)$ and $B(\Gamma)$ are defined as

$$\begin{aligned} A(\Gamma) &= \frac{(1 - f_a)(1 - g(1 - q))^2}{2(1 - g) + (2g - 1)(f_a + q) - 2gqf_a}, \\ B(\Gamma) &= \frac{(1 - q)(1 - g(1 - f_a))^2}{2(1 - g) + (2g - 1)(f_a + q) - 2gqf_a}. \end{aligned}$$

Finally, the last equation governs the Γ dependence of N_w :

$$\frac{dN_w}{d\Gamma} = -[P_w^0 + (1 - q)(1 - f_a)g^2 P_s^0 + f_a P_o^0]N_w. \quad (6)$$

Some comments are in order before we go any further with our analysis: First of all, the very fact that these equations can be written down at all relies on the fact that of our ansatz, Eqn (3) for the mass distribution and relative abundances of various clusters, is consistent with the action of the RG transformation. Another thing to notice is that Eqns (4,5) are invariant under the simultaneous interchange of P_s and P_w on the one hand, and f_a and q on the other. This is to be expected, and is related to the $\delta \rightarrow -\delta$ duality of the original problem. Indeed, if we consider interchanging P_s and P_w , which would correspond to the s type bonds being chosen *weaker* than the w type bonds, then our definition of the clusters would no longer be appropriate. In this case, it is more appropriate to think in terms of the complementary clusters enclosing w -type even bonds, and linked together by s -type even bonds. In this complementary description, the roles of f_a and q will clearly be interchanged. Nevertheless, the $\delta \rightarrow -\delta$ duality implies that the equations governing the flows in these complementary variables should have the *same form* as our earlier equations—in other words, the original equations must be form-invariant under a simultaneous interchange of P_s and P_w , and f_a and q . In the rest of the article, I therefore conform without any loss of generality to this suggestive labeling, and restrict attention to situations in which the s -type even bonds are on average stronger than the w -type even bonds, and δ is positive.

The next order of business is clearly to check our effective model and equations against the results of Ref 6 for the special $\delta = 0$ case. Let us begin by setting $P_s \equiv P_w = P_e$, since there is no distinction at all between the w -type and s -type even bonds at $\delta = 0$. Next, note that the average number of s -type even bonds is given by $(1 - f_a)(1 - q)N_w \sum_{\mu=0}^\infty (\mu + 1)q^\mu = N_w(1 - f_a)/(1 - q)$. Requiring that this equal N_w gives the expected result: $f_a = q$ at $\delta = 0$. This immediately implies that the total number of antiferromagnetically coupled odd pairs of spin-1/2s equals $2f_a N_w$. Furthermore, the number of ferromagnetically coupled odd pairs is expected to equal that of the antiferromagnetically coupled odd pairs on average. This implies that $f_a = (2N_{ff} + N_{1f})/2N_w = (1 - f_a)(1 - g)$. Moreover, the ratio N of the number of spin-1s to the number of even bonds in the system (the notation is chosen to conform with that of Ref 6) can be expressed as: $N = (2N_{11} + N_{1f})/2N_w = (1 - f_a)g$. Putting all this together, we can express f_a , g and q in terms of the single parameter N : $f_a = q = (1 - N)/2$, $g = 2N/(1 + N)$. Furthermore, it is easy to check that Eqns (4,5) at $\delta = 0$ are consistent with these relations, and reduce to three independent equations, two for the two functions P_e and P_o , and one for the ratio N . In

fact, a little algebra shows that these reduced equations are *completely equivalent* to the equations of Ref 6.

The fixed points found in Ref 6 can now be translated into our language as follows: To begin with, the RS₁ phase boundary at $R > R_c(\delta = 0)$ is controlled by:

$$\begin{aligned} q &= f_a \equiv (1 - N)/2 = 0, \\ g &\equiv 2N/(1 + N) = 1, \\ P_s(\beta|\Gamma) &= P_w(\beta|\Gamma) = \frac{1}{\Gamma}e^{-\beta/\Gamma}, \\ P_o(\beta|\Gamma) &= Qe^{-Q\beta}, \end{aligned} \quad (7)$$

where Q is an arbitrary constant. [Of course, this is not really a fixed point for the probability distributions P_s and P_w , but becomes one if we transform to a description in terms of the distributions of the scaled variable $\zeta = \beta/\Gamma$; I will be sloppy about such terminology here and below, since it is always clear what is meant from the context]. At such a fixed point, Eqn (6) correctly^{6,7} predicts $N_w \sim \Gamma^{-2}$.

On the other hand, the fixed points describing the $\delta = 0$ Gapless Haldane phase are written as:

$$\begin{aligned} q &= f_a \equiv (1 - N)/2 = 1/2, \\ g &\equiv 2N/(1 + N) = 0, \\ P_s(\beta|\Gamma) &= P_w(\beta|\Gamma) = Pe^{-P\beta}, \\ P_o(\beta|\Gamma) &= Qe^{-Q\beta}, \quad Q = 0, \end{aligned} \quad (8)$$

with P an arbitrary constant; at any such fixed point, Eqn (6) implies $N_w \sim e^{-\Gamma}$, which is consistent with the previous results.^{6,7}

Finally, the multicritical point at $R = R_c, \delta = 0$ is controlled by

$$\begin{aligned} q &= f_a \equiv (1 - N)/2 = 1/4, \\ g &\equiv 2N/(1 + N) = 2/3, \\ P_s(\beta|\Gamma) &= P_w(\beta|\Gamma) = \frac{2}{\Gamma}e^{-2\beta/\Gamma}, \\ P_o(\beta|\Gamma) &= \frac{2}{\Gamma}e^{-2\beta/\Gamma}, \end{aligned} \quad (9)$$

with Eqn (6) again correctly^{6,7} predicting $N_w \sim \Gamma^{-3}$.

Let us now look for new fixed points that would correspond to the rather unusual Griffiths phases we expect to find in the general $\delta > 0$ case. Consider first the (1,1) Griffiths phase at $\delta \neq 0$: In this phase, we expect the odd bonds in the effective model to be much weaker than both types of even bonds (this would guarantee that the resulting pattern of singlet bonds at long length-scales would have the topological order characteristic of the (1,1) phase). Moreover, we expect the typical mass of clusters to scale to zero at low-energies. Guided by such considerations, it is easy to see that our equations admit the following two-parameter family of fixed point solutions that have all the ‘right’ properties:

$$f_a = 1,$$

$$\begin{aligned} q &= g = 0, \\ P_s(\beta|\Gamma) &= P_s e^{-P_s\beta}, \\ P_w(\beta|\Gamma) &= P_w e^{-P_w\beta}, \\ P_o(\beta|\Gamma) &= Qe^{-Q\beta}, \quad Q = 0, \end{aligned} \quad (10)$$

where P_s and P_w are two otherwise arbitrary positive constants that obey $P_s > P_w$ (this condition matters for the stability of these fixed points). [Note that using these fixed point values in Eqn (6) implies $N_w \sim e^{-P_w\Gamma}$.]

Similarly, in the (2,0) Griffiths phase, we expect the w -type even bonds to be much weaker than either the s -type even bonds or the odd bonds. In addition, we again expect the masses of clusters to go to zero at low-energies. Furthermore, from the physical picture developed earlier, we expect that there are two distinct regions in this Griffiths phase, a spin-1/2 rich region closer to the RS_{1/2} phase boundary, and a spin-1 rich region adjacent to the RS₁ phase boundary. Again, it is not hard to find the corresponding two-parameter families of fixed points. The region closer to the RS_{1/2} phase boundary is controlled by:

$$\begin{aligned} f_a &= g = 1, \\ q &= 0, \\ P_s(\beta|\Gamma) &= P_s e^{-P_s\beta}, \\ P_o(\beta|\Gamma) &= P_o e^{-P_o\beta}, \\ P_w(\beta|\Gamma) &= Qe^{-Q\beta}, \quad Q = 0, \end{aligned} \quad (11)$$

where P_s and P_o are otherwise arbitrary positive constants satisfying $P_s > P_o$ (again this controls the stability of these fixed points). [Note that using these fixed point values in Eqn (6) implies $N_w \sim e^{-P_o\Gamma}$.]

On the other hand, the region closer to the RS₁ phase boundary is controlled by:

$$\begin{aligned} f_a &= q = 0, \\ g &= 1, \\ P_s(\beta|\Gamma) &= P_s e^{-P_s\beta}, \\ P_o(\beta|\Gamma) &= P_o e^{-P_o\beta}, \\ P_w(\beta|\Gamma) &= Qe^{-Q\beta}, \quad Q = 0, \end{aligned} \quad (12)$$

with $P_s < P_o$ in this case (as before, this is related to the stability of these fixed points). [Note that using these fixed point values in Eqn (6) implies $N_w \sim e^{-P_s\Gamma}$.]

Furthermore, for the ‘degenerate’ crossover case characterized by $P_s = P_o$, we have an additional degree of freedom in the choice of f_a . Of course, for any physical system, both f_a and the common value, P , of P_s and P_w will be determined by complicated physics at higher energies—the corresponding functional relationship between the two along the cross-over line in (R, δ) plane is clearly outside the scope of our analysis, although we will see later that it is possible to predict the leading behavior of both f_a and P_s as one approaches the multicritical point along the crossover line. [Also, note that the non-universal value of f_a along this line of fixed points

does *not* affect the scaling of N_w , with Eqn (6) predicting $N_w \sim e^{-P\Gamma}$]

Finally, the $RS_{1/2}$ phase boundary is described by the last specimen in our menagerie of fixed points:

$$\begin{aligned} f_a &= 1, \\ q &= 0, \\ g &= 1/2, \\ P_s(\beta|\Gamma) &= P_s e^{-P_s\beta}, \\ P_w(\beta|\Gamma) &= P_o(\beta|\Gamma) = \frac{1}{\Gamma} e^{-\beta/\Gamma}, \end{aligned} \quad (13)$$

with P_s an arbitrary positive constant. [Note that using these fixed point values in Eqn (6) implies $N_w \sim \Gamma^{-2}$, as expected.]

V. SCALING FLOWS AND CROSSOVERS

Naturally, the low-energy physics in any regime depends on the fixed point controlling it via the scaling flows and crossovers in the vicinity of the fixed point, and it is crucial to characterize these in order to develop a complete picture of the low-energy behavior.

A. Near the Multicritical point

Let us begin in the neighborhood of the multicritical point. From the $\delta = 0$ analysis of Ref 6, we know that the flows away from this point along the R axis are controlled by the relevant eigenvalue $\lambda_r = (\sqrt{13} - 1)/2$. A more general stability analysis should yield another relevant eigenvalue λ_δ , reflecting the expected instability of this fixed point to infinitesimal dimerization. Together, these two exponents will then control the multicritical scaling near this point in the usual way; in particular, the ratio λ_r/λ_δ will determine the shape of the $RS_{1/2}$ phase boundaries asymptotically close to the multicritical point.

Following Refs 8,6, let us look for eigenperturbations of the form

$$\begin{aligned} P_s(\beta|\Gamma) &= P_s^{\text{fp}}(\beta|\Gamma) + 2(\epsilon_e + \epsilon_{sw})\Gamma^{\lambda-1} \left(1 - \frac{2\beta}{\Gamma}\right) e^{-2\beta/\Gamma}, \\ P_w(\beta|\Gamma) &= P_w^{\text{fp}}(\beta|\Gamma) + 2(\epsilon_e - \epsilon_{sw})\Gamma^{\lambda-1} \left(1 - \frac{2\beta}{\Gamma}\right) e^{-2\beta/\Gamma}, \\ P_o(\beta|\Gamma) &= P_o^{\text{fp}}(\beta|\Gamma) + 2\epsilon_o\Gamma^{\lambda-1} \left(1 - \frac{2\beta}{\Gamma}\right) e^{-2\beta/\Gamma}, \\ f_a &= f_a^{\text{fp}} + (\epsilon_{aq} - \epsilon_n/4)\Gamma^\lambda, \\ q &= q^{\text{fp}} - (\epsilon_{aq} + \epsilon_n/4)\Gamma^\lambda, \\ g &= g^{\text{fp}} + (4\epsilon_n/9 + 2\epsilon_g/3)\Gamma^\lambda, \end{aligned} \quad (14)$$

where the superscript fp denotes the values at the multicritical fixed point. In the above, the coefficients ϵ have been chosen so as to separate out the effects of going

away from $\delta = 0$ from the effects of changing R at $\delta = 0$; thus, $\epsilon_{aq} = \epsilon_g = \epsilon_{sw} = 0$ if δ remains zero. Conversely, ϵ_n and ϵ_e are both expected to be zero if R remains at its multicritical value. ϵ_o is the only coefficient that can, in principle, get contributions both from deviations in R at $\delta = 0$, and from deviations in δ for R fixed at its multicritical value. However, one expect on physical grounds that the distributions of the odd bonds, related as it is to the effective couplings between the end-spins of a long segment in the Haldane phase, is relatively insensitive to δ so long as it is small—it is therefore reasonable to assume that ϵ_o is zero to linear order in δ at fixed R . [In other words, the coefficients ϵ are related to the perturbations in δ and R as $\epsilon_o = c_o r + \dots$, $\epsilon_e = -c_e r + \dots$, and $\epsilon_{sw} = c_{sw} \delta + \dots$, $\epsilon_{aq} = c_{aq} \delta \dots$ and $\epsilon_n = c_n r + \dots$, with all the c being positive and $0(1)$, and $r \equiv R - R_c(0)$.]

This ansatz is readily seen to solve the flow equations to linear order in the ϵ , provided the following system of linear equations is satisfied:

$$\begin{aligned} \lambda\epsilon_g &= -5\epsilon_g, \\ \lambda\epsilon_n &= 3\epsilon_g - \frac{3}{2}\epsilon_n - \frac{3}{2}\epsilon_e + \frac{3}{2}\epsilon_o, \\ \lambda\epsilon_e &= -\epsilon_g - \frac{1}{2}\epsilon_n - \frac{1}{2}\epsilon_e - \frac{1}{2}\epsilon_o, \\ \lambda\epsilon_o &= \epsilon_g + \epsilon_n - \epsilon_e, \\ \lambda\epsilon_{aq} &= -\frac{3}{2}\epsilon_{aq} + \frac{9}{8}\epsilon_{sw}, \\ \lambda\epsilon_{sw} &= 2\epsilon_{aq} + \frac{1}{2}\epsilon_{sw}. \end{aligned} \quad (15)$$

Fortunately, all eigenvalues of this system can be easily determined as follows: To begin with, we can set $\epsilon_g = \epsilon_{aq} = \epsilon_{sw} = 0$, to obtain the three eigenvalues -1 , $-(1 + \sqrt{13})/2$, and $\lambda_r \equiv (\sqrt{13} - 1)/2$ that characterize the $\delta = 0$ flows; the corresponding eigenvectors live entirely in the $(\epsilon_e, \epsilon_o, \epsilon_n)$, and correspond precisely to the eigenperturbations described in Ref 6. Next, note that $\lambda = -5$ is clearly an eigenvalue; the corresponding eigenvector has $\epsilon_{aq} = \epsilon_{sw} = 0$ and lives entirely in the $(\epsilon_g, \epsilon_n, \epsilon_e, \epsilon_o)$ subspace. Finally, we have two eigenvectors that live entirely in the $(\epsilon_{aq}, \epsilon_{sw})$ subspace, with eigenvalues $-(1 + \sqrt{13})/2$ and $\lambda_\delta \equiv (\sqrt{13} - 1)/2$. Thus, we indeed have just two relevant eigenvalues, the first λ_r corresponding to moving along the R axis at $\delta = 0$, and the other λ_δ representing the effects of non-zero dimerization at $R = R_c(\delta = 0)$. The important, and at first sight rather surprising, feature is that these two eigenvalues are equal! In actual fact, this equality reflects an underlying S_3 (permutation group of three elements) symmetry of the multicritical point (corresponding to free interchange between the three phases that meet at this point); a discussion of this point, as well as generalizations to some closely related problems, is the subject of a separate article.¹³

Now, a reasonable picture of the full crossover from the multicritical point to any of the phases in its vicinity is to assume that a system very close to the multicritical point

follows the multicritical flows as the RG proceeds *until either* $r\Gamma^{\lambda_r}$ *or* $\delta\Gamma^{\lambda_\delta}$ *becomes* $O(1)$, after which the system obeys the scaling flows characteristic of the fixed point governing the phase it is in. This matching procedure can then be used to relate the scaling behavior of various quantities near the multicritical point to the two relevant eigenvalues λ_r and λ_δ , and I will have more to say along these lines after we analyze the low-energy behavior of the different phases. For now, let us ask a more basic question, namely, the shape of the $RS_{1/2}$ phase boundaries close to the multicritical point. It is convenient to formulate the argument in terms of the scaling behavior of the some physical property, such as the *topological order parameter*⁷ $T \equiv \lim_{\Gamma \rightarrow \infty} T(r, \delta, \Gamma)$ that characterizes the connectivity property of the (1,1) phase (see Ref 7 for the precise definition). Multicritical scaling, in conjunction with the results of Ref 7 for $\delta = 0$, implies that we may write

$$T(r, \delta, \Gamma) = \Gamma^{-(6-2\phi_M)} F(r\Gamma^{\lambda_r}, \frac{\delta^{\lambda_r}}{r}), \quad (16)$$

with $\lim_{x \rightarrow -\infty} F(x, 0) \sim |x|^{\frac{6-2\phi_M}{\lambda_r}}$, $F(0, 0)$ a constant, and $\phi_M = \sqrt{5}$. Now, if we keep r fixed at some small negative value and increase δ from zero, the presence of the $RS_{1/2}$ phase boundary at which the topological order is lost must be reflected in the the large Γ limit of F . Indeed, as we will see in the next section, one expects $T(\Gamma)$ to scale as $\Gamma^{-(4-2\phi_{RS})}$ on the $RS_{1/2}$ phase boundary, with $\phi_{RS} = (\sqrt{5} + 1)/2$. This can be consistent with the multicritical scaling form F only if $\lim_{x \rightarrow -\infty} F(x, -y_c) \sim x^{(3-\sqrt{5})/\lambda_r}$ for some particular $y_c > 0$, implying that $\delta^{\lambda_r} = -y_c r$ is the equation for the $RS_{1/2}$ phase boundary close to the multicritical point. Since we have $\lambda_r = \lambda_\delta$, this means that the phase boundary comes in *linearly* as shown in the schematic phase diagram Fig 1. Of course, Fig 1 contains another ingredient, namely that the $RS_{1/2}$ line slopes *downwards*, ruling out reentrant behavior. To justify this needs a somewhat more detailed consideration of the actual crossovers—while it is possible to do this using eigenvector information and the matching procedure outlined above, I do not pursue this further here.

B. Near the $RS_{1/2}$ and RS_1 phase boundaries

The analysis in the vicinity of the $RS_{1/2}$ and RS_1 fixed lines is much simpler, and the two cases are closely analogous. Here, I discuss only the $RS_{1/2}$ phase boundary in detail, confining myself to a brief summary of the corresponding results in the RS_1 case.

In order to study small perturbations around a point on the $RS_{1/2}$ line, it is convenient to parametrize these deviations as

$$P_s(\beta|\Gamma) = P_s e^{-P_s \beta} [1 + \delta_s (1 - P_s \beta)],$$

$$\begin{aligned} P_w(\beta|\Gamma) &= \frac{e^{-\beta/\Gamma}}{\Gamma} [1 + (\delta_p - \delta_{ow})(1 - \frac{\beta}{\Gamma})], \\ P_o(\beta|\Gamma) &= \frac{e^{-\beta/\Gamma}}{\Gamma} [1 + (\delta_p + \delta_{ow})(1 - \frac{\beta}{\Gamma})], \\ g &= \frac{1}{2}(1 + \delta_g), \\ f_a &= 1 - \delta_a, \\ q &= \delta_q. \end{aligned} \quad (17)$$

Requiring that this ansatz satisfy the linearized flow equations yields a linear system of ordinary differential equations for the functions $\delta(\Gamma)$. Fortunately, the equations for δ_a and δ_q are particularly simple:

$$\begin{aligned} \frac{d\delta_a}{d\Gamma} &= -(P_s - \frac{2}{\Gamma})\delta_a, \\ \frac{d\delta_q}{d\Gamma} &= -(P_s + \frac{1}{\Gamma})\delta_q + \frac{3\delta_a}{4\Gamma}. \end{aligned} \quad (18)$$

These immediately fix the Γ dependence of δ_a and δ_q to be

$$\begin{aligned} \delta_a &= C_a \Gamma^2 e^{-P_s \Gamma}, \\ \delta_q &= (\frac{C_a \Gamma^2}{4} + \frac{C_q}{\Gamma}) e^{-P_s \Gamma}; \end{aligned} \quad (19)$$

at large Γ , both δ_a and δ_q thus decay extremely rapidly to zero (compared to the Γ^λ behavior we anticipate for δ_{ow} , δ_p , and δ_g). Furthermore, it is easy to check that the linearized equation for δ_s only involves δ_q and δ_a :

$$\frac{d\delta_s}{d\Gamma} = -\frac{\delta_q}{\Gamma} - \frac{\delta_a}{4\Gamma}, \quad (20)$$

which implies that the leading large Γ behavior of δ_s is

$$\delta_s(\Gamma) \sim \text{const.} + \frac{C_a \Gamma}{2P_s} e^{-P_s \Gamma}. \quad (21)$$

The presence of the constant term in the above merely reflects the fact that we have a whole line of $RS_{1/2}$ fixed points with $P_s(0|\Gamma)$ varying continuously along the line (in RG terms, this is a marginal coupling); requiring that the fixed point value of $P_s(0|\Gamma)$ be P_s at the particular point about which we are perturbing tunes the constant to zero, implying that δ_s also decays very rapidly at large Γ .

This simplifies matters considerably—for clearly, we are at liberty to set δ_a , δ_s , and δ_q to zero in the linearized equations for δ_{ow} , δ_p , and δ_g in order to determine the eigenvalues λ that control the slow growth or decay of these perturbations. The corresponding linearized equations (with the $\delta_{a/q/s}$ set to zero) read:

$$\begin{aligned} \frac{d\delta_g}{d\Gamma} &= \frac{1}{\Gamma}(2\delta_{ow} - 2\delta_g), \\ \frac{d\delta_p}{d\Gamma} &= -\frac{\delta_p}{\Gamma}, \\ \frac{d\delta_{ow}}{d\Gamma} &= +\frac{\delta_{ow}}{\Gamma} \end{aligned} \quad (22)$$

As in the previous section, the eigenmodes are clearly of the form $\delta_{g/p/ow} = \epsilon_{g/p/ow}\Gamma^\lambda$, with the coefficients ϵ constrained by

$$\begin{aligned}\lambda\epsilon_p &= -\epsilon_p, \\ \lambda\epsilon_{ow} &= +\epsilon_{ow}, \\ \lambda\epsilon_g &= -2\epsilon_g + 2\epsilon_{ow}.\end{aligned}\quad (23)$$

The three eigenvalues are $+1$, -1 , and -2 , with the respective eigenvectors proportional to $(\epsilon_p = 0, \epsilon_{ow} = 1, \epsilon_g = 2/3)$, $(\epsilon_p = 1, \epsilon_{ow} = 0, \epsilon_g = 0)$, and $(\epsilon_p = 0, \epsilon_{ow} = 0, \epsilon_g = 1)$.

Thus, as expected, there is a single relevant eigenperturbation on the $RS_{1/2}$ line. Clearly, this corresponds to tuning the bare dimerization away from the critical value $\delta = \delta_c$; from the form of the relevant eigenvector, it is clear that this gives rise to a slight imbalance in the strengths of the w -type even bonds and the odd bonds in the effective model, which in turn drives g away from its critical value of $1/2$ (as it must, since the fixed point value of g is 1 in the $(2,0)$ phase, and 0 in the $(1,1)$ phase). This analysis also allows us to identify the appropriate crossover energy scale for a system close to the $RS_{1/2}$ phase boundary—clearly, any such system will ‘look’ critical for Γ less than the log-energy scale $\Gamma_{\delta_{\text{eff}}} \sim \delta_{\text{eff}}^{-1}$, and will have behavior characteristic of either the $(2,0)$ or $(1,1)$ phase for Γ greater than this crossover scale (here $\delta_{\text{eff}} \equiv \delta - \delta_c$). All of the above is clearly identical to the original analysis of the spin-1/2 chain,^{8,14} and thus, the analysis here confirms the heuristic picture of Section II. Moreover, this also makes it clear that scaling behavior of the topological order parameter T in the vicinity of the $RS_{1/2}$ phase boundary will be identical to the behavior of the dimerization order parameter¹⁴ in the random spin-1/2 HAF chain in the vicinity of its $RS_{1/2}$ critical point at zero dimerization; in particular, one therefore expect that $T(R = R_c, \delta = \delta_c, \Gamma) \sim \Gamma^{(4-2\phi_{RS})}$ on our $RS_{1/2}$ phase boundary, with $\phi_{RS} = (\sqrt{5} + 1)/2$.¹⁶

The analysis near the RS_1 line proceeds similarly: From the linearized flow equations, it is easy to establish that perturbations in the values of g , f_a , and q all die away exponentially (apart from some unimportant prefactors of powers of Γ) at large Γ . Furthermore, $P_o(\beta|\Gamma)$ also settles down to its fixed point form just as rapidly (of course, $P_o(0|\Gamma)$ is now a marginal coupling along this line, and the particular value P_o it settles down to depends on the initial condition, analogous to the behavior of P_s in the $RS_{1/2}$ case above). This means we are at liberty to set all of these variables to their fixed point values in our analysis of the much slower ($\sim \Gamma^\lambda$) growth or decay of perturbations of P_s and P_w away from their common fixed point form. Using the usual parametrization,

$$\begin{aligned}P_s(\beta|\Gamma) &= \frac{1}{\Gamma} e^{-\frac{\beta}{\Gamma}} (1 + (\epsilon_e + \epsilon_{sw})\Gamma^\lambda (1 - \frac{\beta}{\Gamma})), \\ P_w(\beta|\Gamma) &= \frac{1}{\Gamma} e^{-\frac{\beta}{\Gamma}} (1 + (\epsilon_e - \epsilon_{sw})\Gamma^\lambda (1 - \frac{\beta}{\Gamma})),\end{aligned}\quad (24)$$

for these slow deviations makes it clear that we again have precisely one relevant eigenvalue $\lambda = 1$, with the corresponding eigenvector proportional to $(\epsilon_e = 0, \epsilon_{sw} = 1)$ (with the irrelevant eigenvector, of eigenvalue $\lambda = -1$, being proportional to $(\epsilon_e = 1, \epsilon_{sw} = 0)$). Moreover, the relevant perturbation clearly corresponds to turning on a slight dimerization, which introduces an imbalance in the strengths of the s -type and w -type even bonds. Finally, the corresponding crossover energy scale Γ_δ again behaves as $\Gamma_\delta \sim \delta^{-1}$ for small δ , in complete analogy with the spin-1/2 case.

C. In the (1,1) Griffiths phase

As we have seen earlier, the $(1,1)$ Griffiths phase for $\delta \geq 0$ is described by a two-parameter family of fixed points, with $P_s \equiv P_s(0|\Gamma)$ and $P_w \equiv P_w(0|\Gamma)$ allowed to vary independently of each other, modulo the constraint $P_s \geq P_w$. As expected, a formal stability analysis at any point with $P_s > P_w$ yields two marginal eigenperturbations (with $\lambda = 0$) corresponding to these two free parameters, with all other perturbations dying away exponentially in Γ .¹⁹ However, most low energy properties in the phase are controlled by precisely these other terms that decay exponentially in Γ —after all, the exponential decay in the log-energy Γ translates to power-law behavior in the energy Ω , and it is precisely these power-laws that are the characteristic signature of any Griffiths phase.

To analyze the low-energy flows in sufficient detail to get at this behavior, it is useful to parametrize small perturbations away from any $\delta > 0$ fixed point labeled as (P_s, P_w) (with $P_s > P_w$) as

$$\begin{aligned}P_s(\beta|\Gamma) &= P_s e^{-P_s\beta} (1 + \epsilon_s(1 - P_s\beta)), \\ P_w(\beta|\Gamma) &= P_w e^{-P_w\beta} (1 + \epsilon_w(1 - P_w\beta)), \\ P_o(\beta|\Gamma) &= P_o(\Gamma) e^{-P_o(\Gamma)\beta} (1 + \epsilon_o(1 - P_o(\Gamma)\beta)), \\ g &= \epsilon_g, \\ f_a &= 1 - \epsilon_a, \\ q &= \epsilon_q,\end{aligned}\quad (25)$$

with $P_o(\Gamma) \equiv C_o e^{-P_w\Gamma}$ —this choice of $P_o(\Gamma)$ ‘factors’ out the Γ dependence expected ‘at’ the fixed point, with ϵ_o representing a small sub-dominant correction. Moreover, this ansatz clearly satisfies the flow equations to leading order in the ϵ so long as the ϵ obey a corresponding system of ordinary differential equations that governs their Γ dependence.

Now, a simple analysis of the form of these equations reveals that the perturbations ϵ_s , ϵ_w , and ϵ_o and their Γ dependence play no role in determining the leading large Γ asymptotics of ϵ_g , ϵ_a , and ϵ_q . The $\epsilon_{s/w/o}$ can thus be set to zero as far as the analysis of the other perturbations is concerned, and the results of this analysis for $\epsilon_{g/a/q}$ can then be ‘fed back in’ to work out the leading behavior of the $\epsilon_{s/w/o}$ (this latter step is actually quite

unimportant, for it turns out that the low-energy properties of the system depend crucially on the behavior of the $\epsilon_{g/a/q}$, and very little on that of $\epsilon_{s/w/o}$. This simplifies the equations for $\epsilon_{g/a/q}$ considerably, yielding:

$$\begin{aligned}\frac{d\epsilon_a}{d\Gamma} &= -(P_s - P_w)\epsilon_a, \\ \frac{d\epsilon_g}{d\Gamma} &= -P_w\epsilon_g + C_o e^{-P_w\Gamma}, \\ \frac{d\epsilon_q}{d\Gamma} &= -P_s\epsilon_q + P_w\epsilon_a,\end{aligned}\quad (26)$$

where, on the right hand side of each equation, only the terms that matter the most for the large Γ asymptotics have been kept. The solution to these is relatively straightforward to write down:

$$\begin{aligned}\epsilon_a &= C_a e^{-(P_s - P_w)\Gamma}, \\ \epsilon_g &= (\Gamma C_o + C_g) e^{-P_w\Gamma}, \\ \epsilon_q &= C_a (e^{-(P_s - P_w)\Gamma} - C_q e^{-P_s\Gamma}),\end{aligned}\quad (27)$$

where C_a , C_g , and C_q are constants of integration that depend on the initial conditions. Translating from log-energies to the energy scale Ω and keeping only the leading power-law in each case, we thus obtain

$$\begin{aligned}\epsilon_a &\sim \Omega^{P_s - P_w}, \\ \epsilon_g &\sim (C_g + C_o \ln(\Omega_0/\Omega)) \Omega^{P_w}, \\ \epsilon_q &\sim \Omega^{P_s - P_w}.\end{aligned}\quad (28)$$

With this in hand, one can now quite easily work out the leading Γ dependence of $\epsilon_{s/w/o}$; however, as this will play no role in our later discussion, I refrain from displaying the results of this analysis.

To summarize, Eqn 28 implies a rather simple picture for the effective Hamiltonian at cutoff scale Ω : This picture is in terms of type- a clusters, and 0-mass clusters of the 11, 1f, and ff types, all connected to each other by w -type even bonds. Using the leading Ω dependence of N_w , $N_w \sim \Omega^{P_w}$, derived earlier, the abundances of various types of clusters are seen to scale as

$$\begin{aligned}N_a &\sim \Omega^{P_w}, \\ N_{ff} &\sim \Omega^{P_s}, \\ N_{1f} &\sim (C_o \ln(\frac{\Omega_0}{\Omega}) + C_g) \Omega^{P_s + P_w}, \\ N_{11} &\sim (C_o^2 \ln^2(\frac{\Omega_0}{\Omega}) + 2C_g C_o \ln(\frac{\Omega_0}{\Omega}) + C_g^2) \Omega^{P_s + 2P_w},\end{aligned}\quad (29)$$

while the magnitudes of the exchange couplings all obey power-law distributions $P(|J|) \sim |J|^{-1+x}$, with $x = P_s$ for s -type even bonds, $x = P_w$ for w -type even bonds, and $x \sim \Omega^{P_w}$ for the odd bonds. The picture that emerges is thus very similar to the results of the heuristic argument in Section II, with the exponents $z_{1/2}$ and z_1 introduced there given in terms of P_s and P_w as $z_{1/2} = P_w^{-1}$, and $z_1 = (P_s + P_w)^{-1}$ (in making this identification, I am

of course ignoring the multiplicative logarithmic corrections, as well as the sub-dominant power-laws predicted by the more detailed analysis here). Furthermore, since $P_s > P_w$, z_1 is indeed less than $z_{1/2}/2$, exactly as predicted by the earlier Griffiths arguments.

With this in hand, we can now match these low-energy flows with our earlier results for the critical and multicritical flows to develop a reasonably accurate picture of the full crossovers as a function of Ω for a system in the (1,1) phase close to the multicritical point or the $RS_{1/2}$ phase boundary. Consider first a system in the (1,1) phase, but very close to the $RS_{1/2}$ phase boundary (and away from the multicritical point). In this case, the system will look critical for Γ less than the crossover value $\Gamma_{\delta_{\text{eff}}} \sim |\delta_{\text{eff}}|^{-1}$ (with $\delta_{\text{eff}} \equiv \delta - \delta_c$), and then cross over to the flows described above at lower energies (i.e higher Γ). For instance, both $P_o(0|\Gamma)$ and $P_w(0|\Gamma)$ will scale down as Γ^{-1} for Γ above this crossover scale, while $P_s(0|\Gamma)$ will remain roughly constant. Beyond this point, $P_o(0|\Gamma)$ will decay rapidly, $P_o(0|\Gamma) \sim |\delta_{\text{eff}}| e^{-|\delta_{\text{eff}}|(\Gamma - \Gamma_{\delta_{\text{eff}}})}$, while $P_{w/s}(0|\Gamma)$ will both remain roughly fixed at their values at the crossover scale. Thus, the continuously varying exponent $z_{1/2}$ does indeed diverge as we approach the $RS_{1/2}$ phase boundary, scaling as δ_{eff}^{-1} , while z_1 is smooth across the phase boundary. Moreover, applying a similar argument to the function $T(R, \delta, \Gamma)$ yields the scaling behavior of the topological order parameter T close to the $RS_{1/2}$ phase boundary: $T(R, \delta, \Gamma)$ is expected to scale as $\Gamma^{-(4-2\phi_{RS})}$ for $\Gamma > \Gamma_{\delta_{\text{eff}}}$, and remains roughly constant as the energy is lowered further— as a result, $T \equiv \lim_{\Gamma \rightarrow \infty} T(R, \delta, \Gamma)$ will scale as $\Gamma_{\delta_{\text{eff}}}^{-(4-2\phi_{RS})}$ implying

$$T \sim |\delta_{\text{eff}}|^{(4-2\phi_{RS})} \quad (30)$$

in the vicinity of the $RS_{1/2}$ phase boundary.

Next, consider a system in the (1,1) phase for $\delta > 0$, but very close to the multicritical point (the behavior at $\delta = 0$ has already been discussed in Ref 6 and Ref 7). Matching the multicritical flows at higher energies with the asymptotic behavior characteristic of the phase tells us that $P_{s/w/o}(0|\Gamma)$ all satisfy similar scaling forms: $P_{s/w/o}(0|\Gamma) = \Gamma^{-1} K_{s/w/o}(r\Gamma^{\frac{1}{\lambda_r}}, \delta/r)$, where $r = R - R_c(\delta = 0)$, and the second argument of the scaling function is determined by the fact that $\lambda_\delta = \lambda_r$. Furthermore, requiring that this be consistent with the expected behavior in the (1,1) phase immediately implies that $P_s \equiv \lim_{\Gamma \rightarrow \infty} P_s(0|\Gamma)$ and $P_w \equiv \lim_{\Gamma \rightarrow \infty} P_w(0|\Gamma)$ can be written as $P_{s/w} = |r|^{\frac{1}{\lambda_r}} \Phi_{s/w}^-(\delta/|r|)$ when $r < 0$ (also note that the earlier results at $\delta = 0$,^{6,7} imply that $\Phi_{s/w}^-(0)$ must be a finite constant)

In other words, the exponents $z_{1/2}$ and z_1 obey the scaling forms

$$\begin{aligned}z_{1/2} &= \frac{1}{|r|^{1/\lambda_r}} \Xi_{1/2}^-\left(\frac{\delta}{|r|}\right) \\ z_1 &= \frac{1}{|r|^{1/\lambda_r}} \Xi_1^-\left(\frac{\delta}{|r|}\right),\end{aligned}\quad (31)$$

where $\Xi_{1/2}^- = 1/\Phi_w^-$, $\Xi_1^- = 1/(\Phi_s^- + \Phi_w^-)$, and r is assumed negative. Of course, in order to be consistent with our earlier analysis near the $\text{RS}_{1/2}$ phase boundary, the scaling function Φ_w^- must vanish as $|y - y_c|$ when $y \equiv \delta/|r|$ approaches y_c (corresponding to the $\text{RS}_{1/2}$ phase boundary), while Φ_s^- must go smoothly to a constant. Moreover, the present analysis tells us something else: Since this $\text{RS}_{1/2}$ scaling sets in roughly when $|y - y_c| < 1$, the width in δ of the critical regime controlled by the the $\text{RS}_{1/2}$ fixed points vanishes linearly with r as one approaches the multicritical point. Furthermore, if we write $z_{1/2} \sim a_r |\delta - \delta_c|^{-1}$ in the vicinity of the $\text{RS}_{1/2}$ critical line, then the scaling form derived above implies that the amplitude a_r obeys $a_r \sim |r|^{1 - \frac{1}{\lambda_r}}$ as we approach the multicritical point along the $\text{RS}_{1/2}$ phase boundary.

D. In the (2,0) Griffiths phase

The situation in the (2,0) Griffiths phase is quite similar. Except on the crossover line, a formal stability analysis again yields two marginal eigenperturbations, corresponding to the freedom of choice of the two ‘coordinates’ P_s and P_o that parametrize the corresponding family of fixed points.²⁰ Of course, as in the (1,1) case, we need to go beyond such a formal linear stability analysis, and describe the flows in greater detail, to get at the low-energy physics. As before, our task is rendered easier by the fact that the deviations of the probability distributions P_s , P_w , and P_o from their fixed point forms play no role in such an analysis as far as the leading large Γ behavior of the other perturbations is concerned, nor do they matter much in our later calculations of various physical quantities; they may therefore be set to zero in our calculations.

Below, I summarize the results of such an analysis separately for each regime of the (2,0) phase.

1. The spin-1/2 rich regime

It is convenient to parametrize the deviations of f_a , g , and q from their fixed point values as

$$\begin{aligned} f_a &= 1 - \epsilon_a, \\ g &= 1 - \epsilon_g, \\ q &= \epsilon_q. \end{aligned} \quad (32)$$

Using this parametrization in the flow equations for f_a , g , and q (in conjunction with the fixed point form for the distributions $P_{s/w/o}$), it is easy to see that the ϵ obey

$$\begin{aligned} \frac{d\epsilon_a}{d\Gamma} &= -(P_s - P_o)\epsilon_a, \\ \frac{d\epsilon_g}{d\Gamma} &= -P_o\epsilon_g + P_s\epsilon_q + C_w e^{-P_o\Gamma}, \\ \frac{d\epsilon_q}{d\Gamma} &= -(P_s + P_o)\epsilon_q + 2\epsilon_g\epsilon_a C_w e^{-P_o\Gamma}, \end{aligned} \quad (33)$$

where only terms that play a role in determining the leading large Γ asymptotics of the ϵ have been kept. [Note that I have used the fixed point dependence $P_w(0|\Gamma) = C_w e^{-P_o\Gamma}$ of $P_w(0|\Gamma)$ that follows immediately from the flow equation for P_w upon using the fixed point values for all other parameters.] These equations immediately imply

$$\begin{aligned} \epsilon_q &= C_a C_w (C_w \ln^2(\frac{\Omega_0}{\Omega}) + 2C_g \ln(\frac{\Omega_0}{\Omega}) + C_q) e^{-(P_s + P_o)\Gamma}, \\ \epsilon_g &= (C_w \ln(\frac{\Omega_0}{\Omega}) + C_g) e^{-P_o\Gamma}, \\ \epsilon_a &= C_a e^{-(P_s - P_o)\Gamma}, \end{aligned} \quad (34)$$

where C_a , C_q , and C_g are all constants of integration.

This gives a rather simple picture of the low-energy effective Hamiltonian at scale Ω : The description is again entirely in terms of type- a clusters, and 0-mass clusters of the 11, 1f, and ff types, all connected to each other by w -type even bonds. Using the leading Ω dependence of N_w , $N_w \sim \Omega^{P_o}$, derived earlier, the abundances of various types of clusters are readily seen to scale as

$$\begin{aligned} N_a &\sim \Omega^{P_o}, \\ N_{11} &\sim \Omega^{P_s}, \\ N_{1f} &\sim (C_w \ln(\frac{\Omega_0}{\Omega}) + C_g) \Omega^{P_s + P_o}, \\ N_{ff} &\sim (C_w^2 \ln^2(\frac{\Omega_0}{\Omega}) + 2C_g C_w \ln(\frac{\Omega_0}{\Omega}) + C_g^2) \Omega^{P_s + 2P_o}, \end{aligned} \quad (35)$$

while the magnitudes of the exchange couplings all obey power-law distributions $P(|J|) \sim |J|^{-1+x}$, with $x = P_s$ for s -type even bonds, $x \sim \Omega^{P_o}$ for w -type even bonds, and $x = P_o$ for the odd bonds. This is clearly very reminiscent of the heuristic picture of Section II, with the exponents $z_{1/2}$ and z_1 introduced there given in terms of P_s and P_o as $z_{1/2} = P_o^{-1}$, and $z_1 = P_s^{-1}$ (in making this identification, I am of course ignoring the multiplicative logarithmic corrections, as well as the sub-dominant power-laws predicted by the more detailed analysis here).

Thus, as expected, this regime of the (2,0) phase is dual at low-energies to the (1,1) phase that is separated from it by the $\text{RS}_{1/2}$ phase boundary; we can pass from one to the other by interchanging the roles of the w -type even bonds and the odd bonds. Of course, in complete analogy with our earlier analysis of the (1,1) phase, the exponents z_1 and $z_{1/2}$ satisfy the multicritical scaling form Eqn 31, and again, $z_{1/2}$ diverges as $a_r |\delta - \delta_c|^{-1}$ close to the $\text{RS}_{1/2}$ phase boundary, with the amplitude scaling as $a_r \sim |r|^{1 - \frac{1}{\lambda_r}}$ for $r \equiv R - R_c$ small enough.

2. The spin-1 rich regime

It is convenient to parametrize the deviations of f_a , g , and q from their fixed point values as

$$\begin{aligned}
f_a &= \epsilon_a, \\
g &= 1 - \epsilon_g, \\
q &= \epsilon_q.
\end{aligned} \tag{36}$$

Using the fixed point form for the distributions $P_{s/w/o}$ in the flow equations, it is easy to see that the ϵ must satisfy

$$\begin{aligned}
\frac{d\epsilon_g}{d\Gamma} &= -P_o\epsilon_g + P_s\epsilon_q + \epsilon_a C_w e^{-P_s\Gamma}, \\
\frac{d\epsilon_q}{d\Gamma} &= -(P_o + P_s)\epsilon_q + 2\epsilon_g C_w e^{-P_s\Gamma}, \\
\frac{d\epsilon_a}{d\Gamma} &= -(P_o - P_s)\epsilon_a + 2P_s\epsilon_g,
\end{aligned} \tag{37}$$

where only terms that play a role in determining the leading large Γ asymptotics of the ϵ have been kept. [Note that I have used the fixed point dependence $P_w(0|\Gamma) = C_w e^{-P_s\Gamma}$ of $P_w(0|\Gamma)$ that follows immediately from the flow equation for P_w upon using the fixed point values for all other parameters.] These equations immediately imply

$$\begin{aligned}
\epsilon_q &= (C_w^2 C_a \ln^2(\frac{\Omega_0}{\Omega}) + 2C_w C_g \ln(\frac{\Omega_0}{\Omega}) + C_q) e^{-(P_s+P_o)\Gamma}, \\
\epsilon_g &= (C_w C_a \ln(\frac{\Omega_0}{\Omega}) + C_g) e^{-P_o\Gamma}, \\
\epsilon_a &= C_a e^{-(P_o-P_s)\Gamma},
\end{aligned} \tag{38}$$

where C_a , C_q , and C_g are all constants of integration.

Once again, this gives a rather simple picture of the low-energy effective Hamiltonian at scale Ω : As before, the description is entirely in terms of type- a clusters, and 0-mass clusters of the 11, 1f, and ff types, all connected to each other by w -type even bonds. Using the leading Ω dependence of N_w , $N_w \sim \Omega^{P_s}$, derived earlier, the abundances of various types of clusters are readily seen to scale as

$$\begin{aligned}
N_a &\sim \Omega^{P_o}, \\
N_{11} &\sim \Omega^{P_s}, \\
N_{ff} &\sim (C_{wa}^2 \ln^2(\frac{\Omega_0}{\Omega}) + 2C_g C_{wa} \ln(\frac{\Omega_0}{\Omega}) + C_g^2) \Omega^{P_s+2P_o}, \\
N_{1f} &\sim (C_{wa} \ln(\frac{\Omega_0}{\Omega}) + C_g) \Omega^{P_s+P_o},
\end{aligned} \tag{39}$$

where we have defined $C_{wa} \equiv C_w C_a$. The magnitudes of the exchange couplings all obey power-law distributions $P(|J|) \sim |J|^{-1+x}$, with $x = P_s$ for s -type even bonds, $x \sim \Omega^{P_o}$ for w -type even bonds, and $x = P_o$ for the odd bonds. And finally, as in the spin-1/2 rich regime, the exponents $z_{1/2}$ and z_1 introduced in Section II can be expressed in terms of P_s and P_o as $z_{1/2} = P_o^{-1}$, and $z_1 = P_s^{-1}$ (again ignoring multiplicative logarithmic corrections, as well as sub-dominant power-laws).

We may now match our earlier results in the vicinity of the RS₁ phase boundary with this low-energy picture to obtain the scaling of z_1 and $z_{1/2}$ close to the the RS₁ line.

In a system close to the RS₁ line (but not close to the multicritical point), and for $\Gamma < \Gamma_\delta \sim \delta^{-1}$, $P_{s/w/o}(0|\Gamma)$ will both scale as Γ^{-1} , while $P_o(0|\Gamma)$ will stay constant. Beyond this crossover scale, $P_{s/o}(0|\Gamma)$ will both stay roughly constant, while $P_w(0|\Gamma)$ will fall off exponentially with increasing Γ . This immediately implies that $z_{1/2}$ will go smoothly to a constant as one approaches the RS₁ phase boundary, while z_1 will diverge as $|\delta|^{-1}$ —again, this is consistent with the Griffiths arguments in Section II.

The situation is somewhat different close to the multicritical point, with $\delta \neq 0$: In this case, $P_{s/w/o}(0|\Gamma)$ all obey the scaling form introduced earlier, $P_{s/w/o}(0|\Gamma) = \Gamma^{-1} K_{s/w/o}(r\Gamma^{\frac{1}{\lambda_r}}, \delta/r)$. The requirement that the $x \rightarrow +\infty$ limit²¹ of the $K_{s/w/o}(x, y)$ be consistent with the behavior expected in this regime of the (2,0) phase immediately implies that $P_s \equiv \lim_{\Gamma \rightarrow \infty} P_s(0|\Gamma)$ and $P_o \equiv \lim_{\Gamma \rightarrow \infty} P_o(0|\Gamma)$ can be written as $P_{s/o} = r^{\frac{1}{\lambda_r}} \Phi_{s/w}^+(\delta/r)$ when $r > 0$. In other words, the exponents $z_{1/2}$ and z_1 obey the scaling forms

$$\begin{aligned}
z_{1/2} &= \frac{1}{|r|^{1/\lambda_r}} \Xi_{1/2}^+(\frac{\delta}{r}) \\
z_1 &= \frac{1}{|r|^{1/\lambda_r}} \Xi_1^+(\frac{\delta}{r}),
\end{aligned} \tag{40}$$

where $\Xi_{1/2}^+ = 1/\Phi_o^+$, $\Xi_1^+ = 1/\Phi_s^+$, and r is assumed positive. Of course, for this to be consistent with our earlier analysis near the RS₁ phase boundary, we must have $\Phi_o^+(0)$ finite and non-zero, and $\Phi_s^+(x)$ vanishing linearly with x for small x . This also tells us something more about the RS₁ scaling for small r : Clearly, the width in δ of the RS₁ critical region vanishes linearly with r for small r ; furthermore, if we write $z_1 \sim a_r |\delta|^{-1}$ near the RS₁ phase boundary, then the critical amplitude a_r scales as $r^{1-\frac{1}{\lambda_r}}$ for small r .

3. Along the crossover line

The analysis of the crossover case is very similar to that in the two regimes on either side, with only some minor differences. As before, the deviations of the three distributions $P_{s/w/o}$ from their fixed point form plays no role in determining the the decay of the perturbations of g and q from their fixed point values. Furthermore, it is easy to see that the leading large Γ behavior of these perturbations is also independent of precisely how f_a approaches its non-universal fixed point value f .

Parametrizing them as

$$\begin{aligned}
g &= 1 - \epsilon_g \\
q &= \epsilon_q,
\end{aligned} \tag{41}$$

it is easy to see that they obey the following system of equations

$$\begin{aligned}\frac{d\epsilon_g}{d\Gamma} &= -P\epsilon_g + P\epsilon_q + fC_w e^{-P\Gamma}, \\ \frac{d\epsilon_q}{d\Gamma} &= -2P\epsilon_q + 2(1-f)C_w e^{-P\Gamma}\epsilon_g,\end{aligned}\quad (42)$$

where P denotes the common fixed point value of $P_{s/o}(0|\Gamma)$, $C_w e^{-P\Gamma}$ is the fixed point value of $P_w(0|\Gamma)$, and only kept the terms that matter the most at large Γ have been kept. The leading large Γ behavior of ϵ_g and ϵ_q immediately follows:

$$\begin{aligned}\epsilon_q &= (f(1-f)C_w^2\Gamma^2 + 2C_w C_g(1-f)\Gamma + C_q)e^{-2P\Gamma}, \\ \epsilon_g &= (C_g + fC_w\Gamma)e^{-P\Gamma},\end{aligned}\quad (43)$$

where C_g and C_q are constants of integration. This can now be used to determine the manner in which $P_{s/w/o}$ settle down to their fixed point values, as well as follow the approach of f_a to its fixed point value. However, since none of this matters for the leading low-energy behavior of the densities of various clusters, I do not pursue this any further here.

These results for ϵ_g and ϵ_q give a simple picture of the low-energy effective Hamiltonian at scale Ω : As in all the other cases, the description is entirely in terms of type- a clusters, and 0-mass clusters of the 11, 1 f , and ff types, all connected to each other by w -type even bonds. Using the leading Ω dependence of N_w , $N_w \sim \Omega^P$, derived earlier, the abundances of various types of clusters are readily seen to scale as

$$\begin{aligned}N_a &\sim f\Omega^P, \\ N_{11} &\sim (1-f)\Omega^P, \\ N_{ff} &\sim (1-f)(A^2 \ln^2(\frac{\Omega_0}{\Omega}) + 2AC_g \ln(\frac{\Omega_0}{\Omega}) + C_g^2)\Omega^{3P}, \\ N_{1f} &\sim 2(1-f)(A \ln(\frac{\Omega_0}{\Omega}) + C_g)\Omega^{2P},\end{aligned}\quad (44)$$

where the constant A is defined as $A = fC_w$. [Of course, as one moves along the crossover line and approaches the multicritical point, f will tend to the universal multicritical value of $1/4$, and P will vanish with the exponent $1/\lambda_r$.]

VI. PHYSICAL PROPERTIES

This detailed picture of the effective Hamiltonian in various parts of the phase diagram can be used, in principle, to obtain corresponding information about the low-temperature (T) thermodynamics, and the low-frequency, low-temperature dynamics. Below, I focus on the low temperature specific heat and susceptibility, as these provide us with a simple, experimentally verifiable signature of the unusual crossover from spin-1/2 to spin-1 behavior as we tune across the crossover line in the (2,0) phase. [Only the Griffiths phases are discussed, since the behavior at the multicritical point and the RS₁ phase boundary has been analyzed in earlier^{6,7} work, and the

properties of the RS_{1/2} phase boundary are identical to that of a spin-1/2 chain in its Random Singlet state, analyzed earlier by Fisher.⁸]

As in Ref 8, the broad power-law distributions of the couplings in the effective Hamiltonian make it possible for us to treat the low-temperature thermodynamics in a relatively simple way. The basic idea is to run the RG till the cutoff Ω is reduced to be $\Omega_T \sim T$, and recognize that the temperature T dominates over almost all exchange couplings in this renormalized problem with cutoff Ω_T . As a result, the leading low-temperature behavior of the system can be understood in terms of the thermodynamics of free spin-1 and spin-1/2 objects, whose densities are obtained from our earlier results for the abundances of various clusters in the effective Hamiltonian at scale Ω_T .

For instance, in the (1,1) Griffiths phase, the leading contribution to the low-temperature entropy will come from the entropy of the almost free spin-1/2 degrees of freedom that make up the type- a clusters.

$$C_V = T \ln(2) \times 2 \frac{dN_a(\Omega_T)}{dT}, \quad (45)$$

where we have set k_B to one. This implies that the leading temperature dependence of the specific heat will be a non-universal power-law of T : $C_V \sim T^{\frac{1}{z_1/2}}$. These spin-1/2 degrees of freedom also provide the dominant contribution to the zero-field susceptibility:

$$\chi = \frac{g^2}{4T} \times 2N_a(\Omega_T), \quad (46)$$

where g is the gyromagnetic ratio, and we have also set μ_B , the Bohr magneton, to 1. The leading temperature dependence of χ is thus $\chi \sim 1/T^{1-\frac{1}{z_1/2}}$

Forming the ‘Wilson-ratio’ $W = T\chi/g^2C_V$, it is clear that the low-temperature limit of W is

$$W = \mathcal{C}_{1/2} z_{1/2} \quad (47)$$

with the *universal* constant $\mathcal{C}_{1/2} = 1/(4 \ln(2))$ characteristic of a *spin-1/2 system*. Since the spin-1 degrees of freedom are always sub-dominant in this phase, this result holds throughout, and the situation for general $\delta \neq 0$ is thus not very different from that predicted for the $\delta = 0$ case in earlier work.^{6,7}

The (2,0) Griffiths phase, on the other hand, presents some unusual possibilities: Clearly, the above analysis carries over unchanged to the spin-1/2 rich regime of the (2,0) phase, and the Wilson ratio takes the same form as in the (1,1) phase. However, in the spin-1 rich regime, the thermodynamics in the low-temperature limit is dominated by type-11 clusters, and therefore controlled by the exponent z_1 that determines their abundance:

$$C_V = T \ln(3) \times 2 \frac{dN_{11}(\Omega_T)}{dT}, \quad (48)$$

which implies that $C_V \sim T^{\frac{1}{z_1}}$ in the low temperature limit. Similarly, the susceptibility χ may be written as

$$\chi = \frac{2g^2}{3T} \times 2N_{11}(\Omega_T), \quad (49)$$

which implies that $\chi \sim 1/T^{1-\frac{1}{z_1}}$ in the low temperature limit. In other words, we again have power-law dependences similar to the spin-1/2 rich regime, with the Wilson ratio

$$W = C_1 z_1 \quad (50)$$

again proportional to the dominant dynamical exponent. However, the constant of proportionality is now *completely different*, and takes on the *universal* value $2/(3 \ln(3))$ characteristic of a *spin-1 system*. Finally, along the crossover line, one again predicts similar power-law dependences controlled by the common value, z , of z_1 and $z_{1/2}$, but the Wilson ratio will now be completely non-universal, with $W = cz$, and c varying continuously along this line. Thus, the low temperature measurements of the Wilson ratio at different points in the (2,0) phase provide one way of getting at the unusual physics of this phase in which the system looks, at low temperatures, like a spin-1 one chain in one regime, and a spin-1/2 chain in the other. However, since the low temperature thermodynamics is always controlled by the dominant dynamical exponent, a direct experimental handle on the second dynamical exponent at any *particular point* in the phase is lacking. Of course, the first corrections to the leading power-law behavior are also straightforward to calculate, and the experimental data could therefore be fit to such a more detailed formula to obtain the sub-dominant dynamical exponent at any particular point; unfortunately, this would probably not be a particularly compelling test of the theoretical picture presented here.

I conclude with some speculations regarding experiments that could be directly sensitive to physics controlled by the second dynamical exponent: One might imagine that both exponents will leave an imprint on some dynamical property like the inelastic neutron scattering cross-section. However, reasoning as in Ref 22, it is clear that the low-frequency intensity of the main feature in the spectrum (at wavevector π) will again be controlled by the dominant exponent, with the contribution of the sub-dominant degrees of freedom only providing a small correction to this dominant low-frequency behavior. While it is possible that the low-frequency intensity in some other parts of the Brillouin zone might have some signature of these sub-dominant contributions, this is not at all obvious, and remains only a tantalizing possibility for now. Another possibility relates to the fact that strong *ferromagnetic correlations* between some pairs of widely separated spins are present in the ground state in either Griffiths phase. Since the occurrence of such correlations is controlled primarily by the second, sub-dominant exponent, any signature of these in the *static*

structure factor at low-temperatures could also give us a way of directly measuring this exponent. Finally, in a regime in which the spin-1/2s dominate, the most direct way of seeing the spin-1s would be to use some dynamical probe that is preferentially sensitive to spin-1 degrees of freedom, via a ‘selection-rule’ requiring that $\Delta m_z = 2$ for the transitions induced (where m_z is the z projection of the spin quantum number of a state), but again, this has not yet been backed up by any specific calculations.

VII. OUTLOOK AND CONCLUSIONS

Thus, the low-energy behavior of random antiferromagnetic spin-1 chain systems presents a particularly interesting example of Griffiths effects if there is some dimerization in the exchange couplings on average. Indeed, as I have demonstrated above, Griffiths effects in such systems lead to a rather unusual Griffiths phase—in one region of such a phase, the system looks like a spin-1/2 chain at low energies, while it transforms itself into a spin-1 chain in another part of the same phase. Somewhat fortunately, this unusual low-energy behavior may be described in detail, and some concrete experimentally verifiable signatures in the low temperature behavior identified, via an ‘almost-exact’ analytical strong-disorder renormalization group approach. The RG approach presented here yields a detailed picture for the effective Hamiltonian valid at low energies in various parts of the phase diagram, and an intriguing possibility for future work is to use this picture to identify some compelling dynamical signatures of this interesting low-energy physics. Of course, Griffiths phases similar to those described here will exist in higher spin chains as well. Given the recent results of Ref 12, $S = 3/2$ chains are of particular interest in this regard, especially since such Griffiths effects could be important even at relatively low values of randomness in these systems (the Griffiths phases of $S = 3/2$ chains will be discussed in a separate¹⁰ article). Finally, it would be interesting to ask if similar disorder effects may exist in two-dimensional magnets with more than one topologically distinct phases for the pure system.

VIII. ACKNOWLEDGEMENTS

I would like to thank Daniel Fisher for valuable advice, discussions, and encouragement throughout the course of this work, David Huse for useful discussions, as well as collaboration on some closely related work,¹³ and O. Motrunich and G. Zaránd for useful discussions and helpful comments on an earlier draft. I would also like to thank E. Demler, B. Halperin, W. Hofstetter, J. Lidmar, G. Refael, S. Sachdev, and R. da Silva for useful discussions, R. Hyman for sending a copy of the relevant

chapter of his unpublished thesis, and NSF grant DMR-9981283 for financial support.

¹ For an experimental review, see C. Broholm *et al.* in *Dynamical Properties of Unconventional Magnetic Systems*, A. T. Skjeltorp and D. Sherrington (eds.), NATO ASI Series, Kluwer Academic Publishers (1998).

² F. D. M. Haldane, Phys. Rev. Lett. **50**, 1153 (1983).

³ M. den Nijs and L. Rommelse, Phys. Rev. B **40**, 4709 (1989).

⁴ I. Affleck, T. Kennedy, E. H. Lieb, and H. Tasaki, Phys. Rev. Lett. **59**, 799 (1987).

⁵ I. Affleck and F. D. M. Haldane, Phys. Rev. B **36**, 5291 (1987).

⁶ R. Hyman and K. Yang, Phys. Rev. Lett. **78**, 1783 (1997); see also R. Hyman, Ph. D thesis, Indiana University (1996, unpublished).

⁷ C. Monthus, O. Gollineli, and Th. Jolicœur, Phys. Rev. Lett. **79**, 3254 (1997); Phys. Rev. B **58**, 805 (1998).

⁸ D. S. Fisher, Phys. Rev. B **50**, 3799 (1994).

⁹ S. K. Ma, C. Dasgupta, and C. K. Hu, Phys. Rev. Lett. **43**, 1434 (1979); for a more detailed discussion, see also C. Dasgupta and S. K. Ma, Phys. Rev. B **22**, 1305 (1980).

¹⁰ K. Damle, D. A. Huse, and G. Refael, *in preparation*.

¹¹ Note that our effective model bears some resemblance to the model proposed in Ref 12 to analyze the effects of randomness on antiferromagnetic $S = 3/2$ chains, although the physics is quite different.

¹² G. Refael, S. Kehrein, and D. S. Fisher, cond-mat/0111295.

¹³ K. Damle and D. A. Huse, *in preparation*.

¹⁴ R. Hyman, K. Yang, R. N. Bhatt, and S. Girivin, Phys. Rev. Lett. **76**, 839 (1996).

¹⁵ F. Igloi, cond-mat/0108350.

¹⁶ Here, we have used the corrected value of ϕ_{RS} , quoted in a footnote of Ref 6, instead of the value derived earlier in Ref 14; see also Ref 17 below for a ‘percolation’ picture reducing this to Fisher’s original result¹⁸ for the corresponding magnetization exponent of the random transverse field Ising chain.

¹⁷ O. Motrunich, K. Damle, and D. A. Huse, Phys. Rev. B **63**, 224204 (2001).

¹⁸ D. S. Fisher, Phys. Rev. B **51**, 6411 (1995).

¹⁹ The Griffiths phase at $\delta = 0$, with $P_s = P_w$ constitutes a special case—at any point along this line, there is, in addition to two marginal perturbations, a marginally relevant perturbation (growing as a power of Γ), which simply reflects the fact that any point in the (1,1) phase with $\delta > 0$ has $q = 0$, reflecting the extreme paucity of s -type even bonds relative to the w -type even bonds at low enough energies, while, precisely at $\delta = 0$, there is no such distinction between the s -type and w -type even bonds, and $q = 1/2$.

²⁰ Along the crossover line, one has, in addition to the two marginal perturbations generic to the (2,0) phase, another marginally relevant perturbation; this is simply the formal way of saying that f_a is driven to either 1 or 0 as soon as

one moves off the crossover line, while at any point along this line, it takes some non-universal value between these two extremes.

²¹ The $x \rightarrow +\infty$ limit is appropriate because the RS_1 line exists only for $r > 0$.

²² K. Damle, O. Motrunich, and D. A. Huse, Phys. Rev. Lett. **84**, 3434 (2000); see also O. Motrunich, K. Damle, and D. A. Huse, Phys. Rev. B **63**, 134424 (2001).